STUDIA UBB CHEMIA, LXVIII, 3, 2023 (p. 71-98)
(RECOMMENDED CITATION)
DOI:10.24193/subbchem.2023.3.05

HYDROGENOLYSIS OF PALM OIL DERIVED METHYL ESTERS OVER NIOBIUM AND TUNGSTEN BASE CATALYSTS

Mihai MARINESCU[a,*], Dragoș CIUPARU[a], Dorin BOMBOȘ[a], Cristina Maria DUȘESCU-VASILE[a], Roxana Daniela POPOVICI[a], Vasile MATEI[a,*]

ABSTRACT. Vegetable oils are widely available in nature and are one of the most important sustainable feedstocks for biofuel production. W/Pd/γ-Al_2O_3-ZnZSM-5 and Nb/Pd/γ-Al_2O_3-ZnZSM-5 catalysts where prepared, characterized and tested in the hydrogenolysis reaction of palm oil fatty acid esters. The catalysts were characterized by determining the textural characteristics, the thermal stability, and the nature of the acidic sites. The appearance of particle agglomerations was evaluated by scanning electron microscopy (SEM). The resulting reaction products were n-aliphatic hydrocarbons, iso-aliphatic hydrocarbons, cycloaliphatic hydrocarbons, and arenes. No oxygenated organic compounds were identified in the collected liquid phase. At lower pressures, the deoxygenation process occurs to approximately 33% through the hydrogenation of the carboxylic bond and to approximately 67% through decarboxylation/decarbonylation, while at higher pressure than 60 bar the deoxygenation process proceeds preferentially through decarboxylation/ decarbonylation.

Keywords: *fatty acids methyl esters, W/Pd/γ-Al_2O_3-ZnZSM-5, Nb/Pd/γ-Al_2O_3-ZnZSM-5, catalyst, hydrogenolysis*

INTRODUCTION

The world's population is increasing, leading to a higher worldwide energy consumption. One fifth of the total energy consumption is represented by the transportation sector and, the need for fuels will become even larger

[a] *Faculty of Petroleum Refining and Petrochemistry, Petroleum-Gas University of Ploiesti, 39 Bucuresti Blvd., 100680, Ploiesti, Romania*
* *Corresponding authors: mihaimarinescu23@gmail.com, vmatei@upg-ploiesti.ro*

in the future [1]. In this context, an effective and sustainable alternative to conventional fossil fuels are biofuels, obtained by the treatment of biomass. Beyond the obvious advantage of renewability, the development of biofuels from plant biomass can significantly reduce greenhouse gas emissions and can bring enormous benefits from both, economic and environmental point of view [2].

Vegetable oils (triglycerides) are widely available in nature and are one of the most important sustainable feedstocks for biofuel production. The biofuel based on fatty acid methyl esters (FAME), is produced by transesterification of triglycerides with methanol with an annual manufacture of more than 20 million tons [3,4]. However, FAME as a transportation fuel has several drawbacks, such as poor calorific value and high viscosity and oxygen content, which obviously limits its application [5].To overcome these limitations, alternative route such as hydrodeoxygenation (HDO) of bio-based feedstock to produce hydrocarbon fuels with high cetane number, low density and viscosity, and easy-blended with traditional fossil fuels was studied [6,7]. The HDO pathway of FAME consist in the hydrogenation of unsaturated fatty acid chains followed by deoxygenation through hydrodeoxygenation, decarbonylation and decarboxylation reactions into a mixture of paraffinic hydrocarbon with chain lengths between C15 and C18. During the reactions, gaseous by-products such as C1-C4 hydrocarbons and CO, CO_2, H_2O are produced [8].

Traditionally, transition metal sulfides catalysts such as Co-Mo and Ni-Mo on Al_2O_3 are used for the hydrotreating processing of triglycerides and fatty acids. However, using sulfide catalysts may lead to contamination of the final product with sulfur residue [9,10]. Another group of catalysts used for the HDO process are noble metal (non sulfided) catalysts, such as Pd, Pt, Rh and Ru, supported mainly on carbon, as well as on Al_2O_3, ZrO_2, CeO_2, TiO_2 have also exhibited high HDO activities [11]. A.R. Ardiyanti et al., [12], reported that Pt, Pd and Rh supported on ZrO_2, Pd/ZrO_2 catalysts exhibited the highest activity, followed by Rh/ZrO2 which however resulted in a product bio-oil with good properties[13]. Shao et al., [14] investigated the hydrodeoxygenation of fatty acid and triglycerides over Nb_2O_5-modified Pd/SiO_2. The results showed an excellent activity and stability for the hydrodeoxygenation of palmitic acid with almost no decrease in hexadecane yield (94–95 %). On the other hand, for hydrocracking reaction, catalysts such as nickel (Ni), niobium phosphate, zeolite, rhodium, platinum, and palladium were tested. Among them, noble metal catalysts (Pd and Pt) are the most favorable for hydrocracking reaction due to their high hydrogenation ability [15].In our previous work [16] a new bi-functional catalyst CuPd/ZSM-5 was developed and tested in the hydrodeoxygenation and hydrocracking reactions of fatty acid methyl esters.

The catalyst led to 100% FAME conversion into n-alkanes, iso-alkanes, saturated and aromatic cyclic hydrocarbons with 9 to 18 carbon atoms. There in order to continue our previous results, in this study, two new tungsten and niobium-based catalysts were prepared and tested for the HDO of fatty acids methyl esters derived from transesterification of palm oil. For better understanding of the reaction mechanisms, kinetic modelling for HDO of fatty acids methyl esters over the two catalysts was performed.

The novel aspects that this study brings refer to the improvement of the catalytic formula to increase the performance of the hydrogenolysis / isomerization / dehydrocyclization process of palm oil derived methyl esters by using ZnZSM5 zeolite in the presence of Nb or W oxides.

RESULTS AND DISCUSSIONS

Textural characteristics of catalysts

The adsorption/desorption isotherms and pore size distribution of the two supported catalysts are presented in Figure 1 and 2, respectively. The adsorption isotherms exhibit a type IV behavior with an H2 hysteresis loops [17-20]. This type of hysteresis loop is characteristic of mesoporous materials with slit-like pores having a narrow distribution of pore body size and a wide distribution of pore entrances.

The volume of nitrogen adsorbed is low up to relative pressures (p/p0) of 0.4, indicating monolayer adsorption at the surface of catalysts. At higher relative pressures, the volume of adsorbed nitrogen increases, and the appearance of the hysteresis loops suggests nitrogen condensation taking place in the interparticle spaces.

The total pore volume determined by the BJH method was 0.309 cm^3/g for the W/Pd/γ-Al_2O_3-ZnZSM5 catalyst with the average pore diameter of 4.2 nm and 0.309 cm^3/g for the Nb/Pd/γ-Al_2O_3-ZnZSM5catalyst with a pore diameter of 4.0 nm.

The surface area, pore volume and average pore diameters of the W/Pd/γ-Al_2O_3-ZnZSM5 and Nb/Pd/γ-Al_2O_3-ZnZSM5 catalysts and of the corresponding support are summarized in Table 1. Impregnation of tungsten, niobium and palladium metals on theγ Al_2O_3-ZnZSM5 support led to a decreased surface area, pore volume and pore diameter.

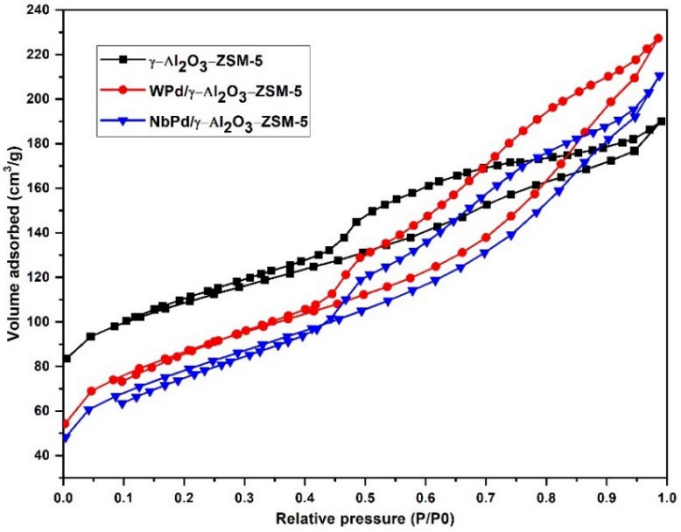

Figure 1. Experimental nitrogen adsorption/desorption isotherm for γ-Al_2O_3-ZnZSM5 support and W/Pd/γ-Al_2O_3-ZnZSM5, Nb/Pd/γ-Al_2O_3-ZnZSM5 catalyst

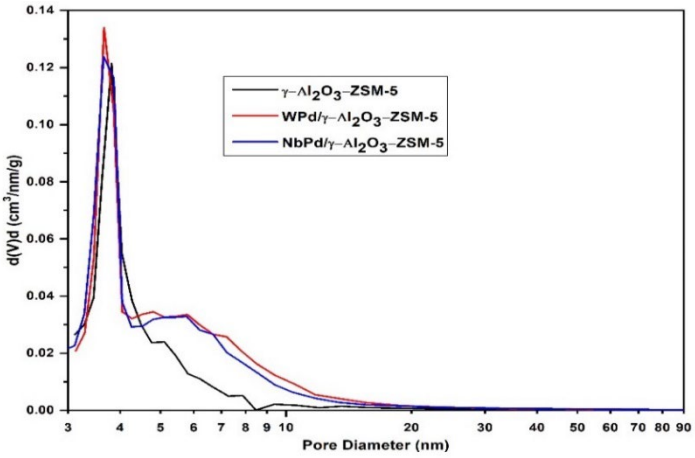

Figure 2. Pore size distribution for γ-Al_2O_3-ZnZSM5 support, W/Pd/γ-Al_2O_3-ZnZSM5 and Nb/Pd/γ-Al_2O_3-ZnZSM5 catalysts

Table 1. Textural characterization for γ-Al_2O_3-ZnZSM5 support and W/Pd/γ-Al_2O_3-ZnZSM5, Nb/Pd/γ-Al_2O_3-ZnZSM5 catalysts

	γ- Al_2O_3-ZnZSM5	W/Pd/γ-Al_2O_3-ZnZSM5	Nb/Pd/γ-Al_2O_3-ZnZSM5
Surface Area, m^2/g	193.38	185.708	184.685
Pore Volume, cm^3/g	0.309	0.283	0.275
Pore Diameter, nm	4.2	3.659	3.650

The Brønsted or Lewis nature of the acidic sites was determined by FTIR pyridine adsorption (Figure 3). The infrared spectra of pyridine at room temperature exhibits three absorption bands at 1540, 1488, and around 1450 cm^{-1}. The Brønsted acid sites correspond to the 1540 cm^{-1} band (pyridinium ion), and the Lewis acid sites to the 1450 cm^{-1} band, attributed to coordinatively bounded pyridine [21,22]. The peak around 1488 cm^{-1} corresponds to the overlapping vibrations of pyridine adsorbed on both Lewis and Brønsted acid sites. Hence, the concentration of both Brønsted and Lewis acid sites was calculated from their corresponding band intensities and extinction coefficients of each type of site using the equation reported by Zhang [21]. The results are presented in Table 2.

Table 2. The acidic properties of γ-Al_2O_3-ZnZSM5 support and W/Pd/γ-Al_2O_3-ZnZSM5, Nb/Pd/γ-Al_2O_3-ZnZSM5 catalysts

Support and catalysts	Lewis acid sites concentration (mmol/g)	Bronsted acid sites concentration (mmol/g)
γ-Al_2O_3-ZSM-5	70.05	15.7
Nb/Pd/γ-Al_2O_3-ZSM-5	90.51 (29.2%)	47.05 (200%)
W/Pd/γ-Al_2O_3-ZSM-5	125.42 (79%)	84.09

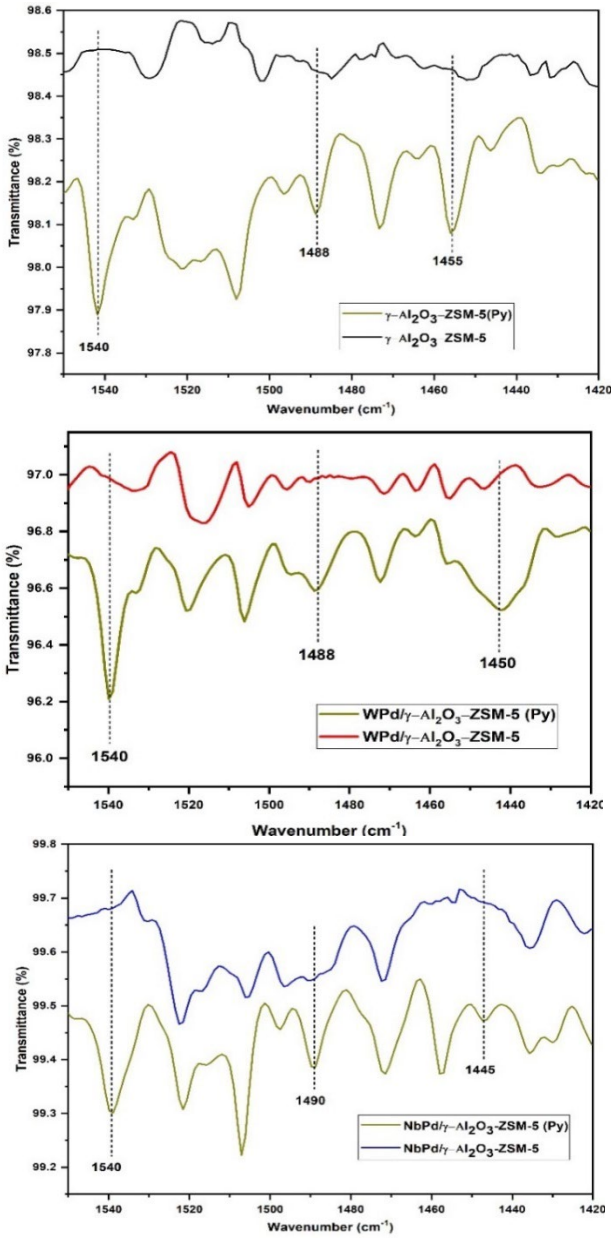

Figure 3. Pyridine-adsorbed FT-IR spectrum of the γ-Al_2O_3- ZnZSM5 support and W/Pd/γ-Al_2O_3- ZnZSM5, Nb/Pd/γ-Al_2O_3- ZnZSM5 catalysts

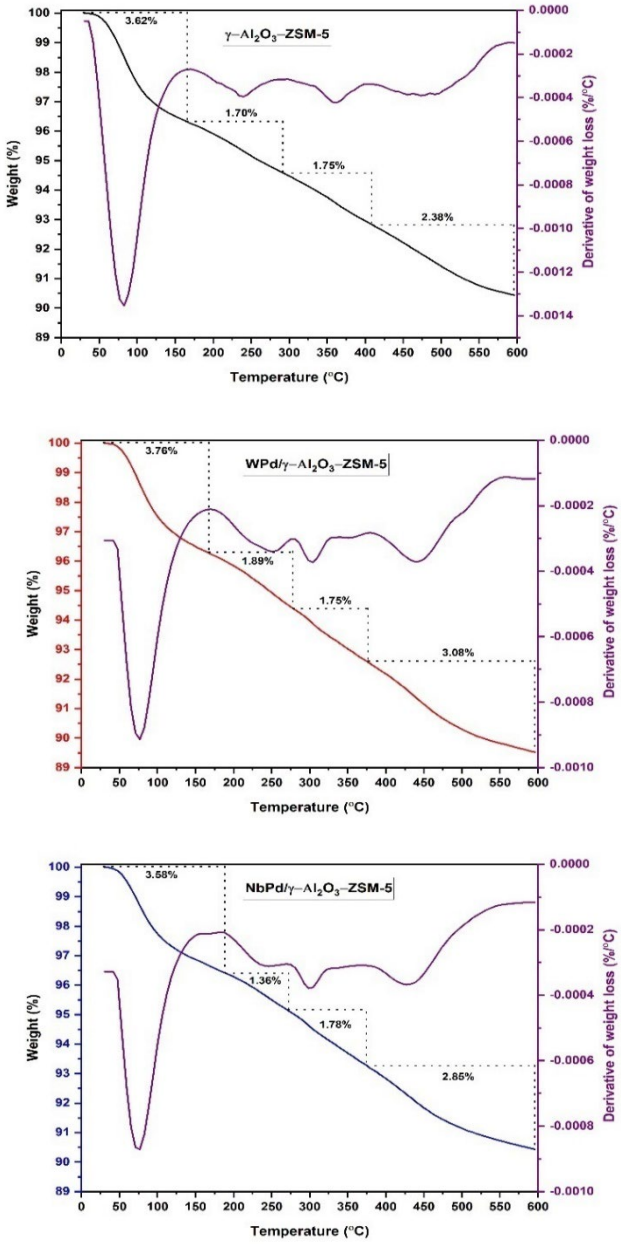

6.3

Figure 4. Thermogravimetric analysis (TGA) and derivative thermogravimetry (DTG) analysis of the support and catalysts

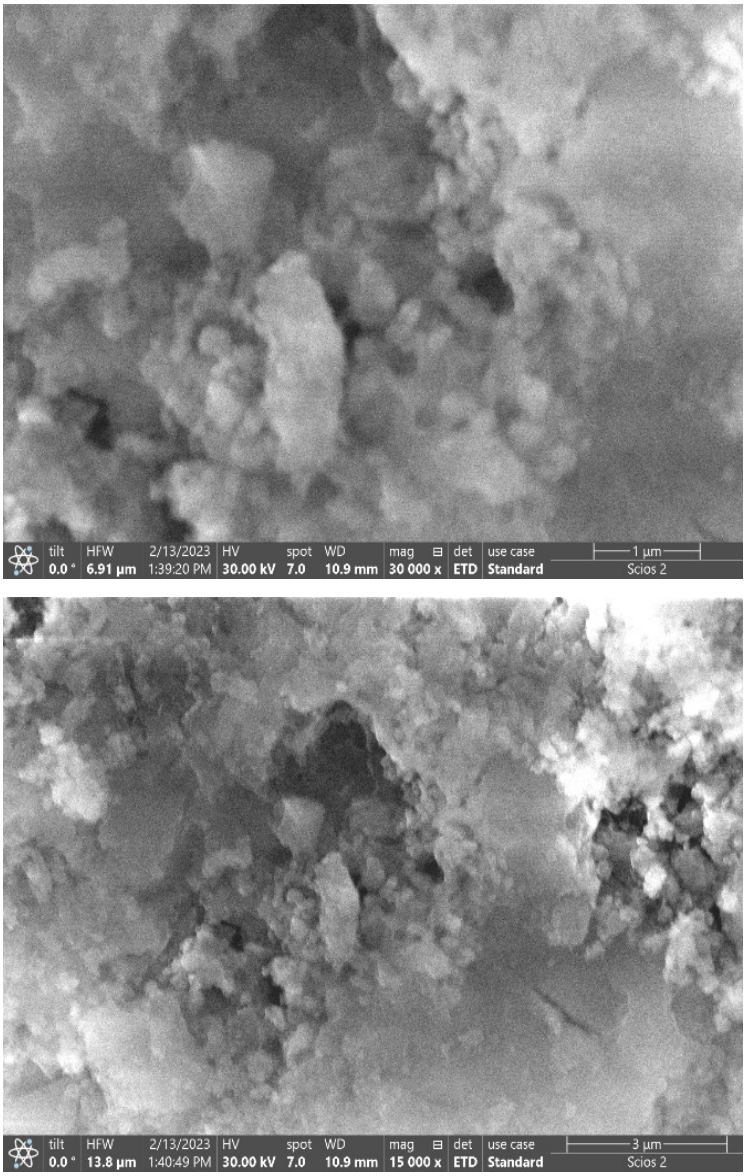

Figure 5. SEM images of the γ-Al_2O_3-ZnZSM5 support

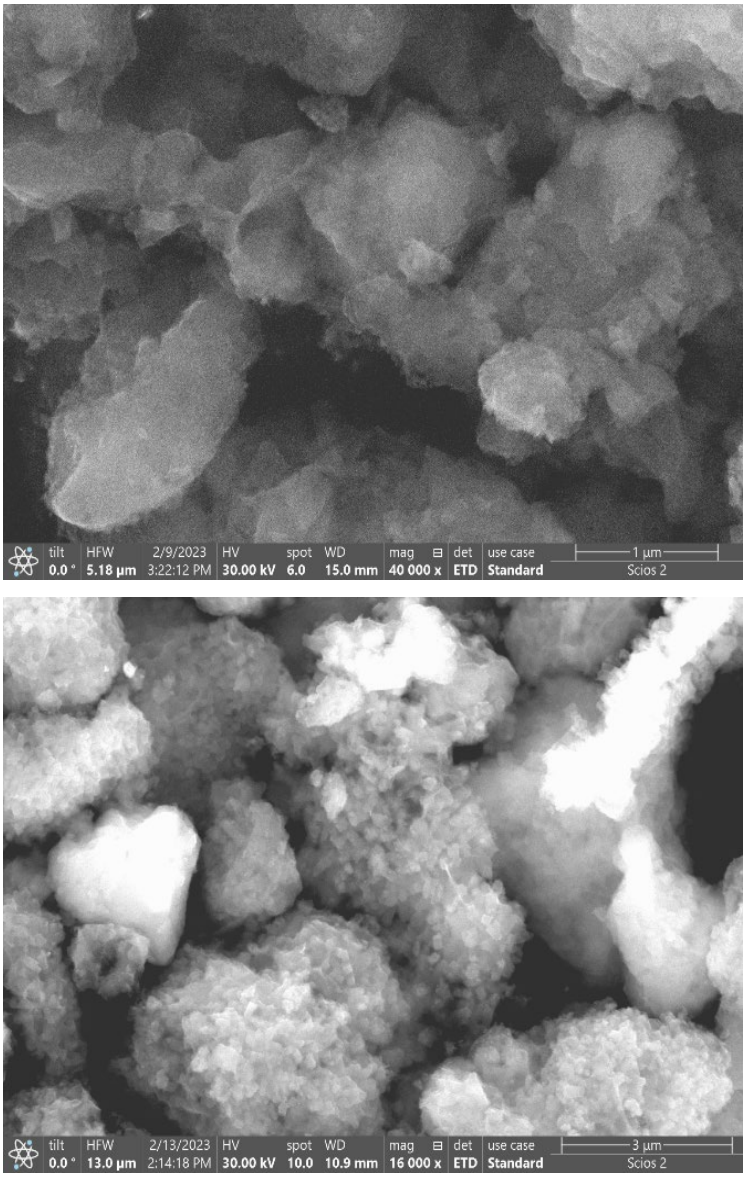

Figure 6. SEM images of the Nb/Pd/γ-Al_2O_3- ZnZSM5 catalyst

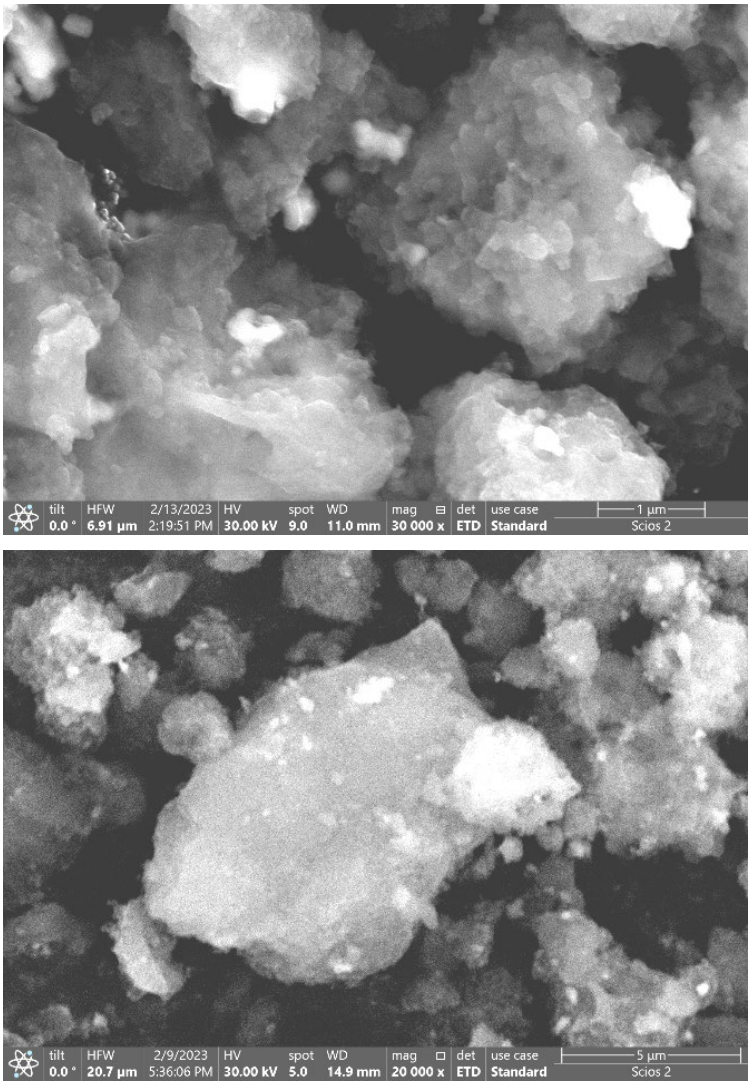

Figure 7. SEM images of the W/Pd/γ-Al_2O_3-ZnZSM5 catalyst

The thermal stability of the catalysts was evaluated to determine the mass losses of the catalytic precursors and their possible chemical changes. The initial weight loss observed in the temperature range of 50°C to 155°C corresponds to the desorption of water molecules [23,24] around 3.62% wt., both for the support and the catalysts (Figure 4). On the derivative thermogravimetric

curve (DTG), multiple mass loss peaks are observed. At higher temperatures, between approximately 200°C and 450°C, the weight loss was 3.45% wt. for the support, 3.64% wt. for the W/Pd/γ-Al_2O_3-ZnZSM5and 3.14% wt. for the Nb/Pd/γ-Al_2O_3- ZnZSM5. This loss can be attributed to the decomposition of the trapped nitrates in the narrow pores of the support and catalysts[25,26]. The slower weight loss of 2.38% wt. for the support, 3.08% wt. for the tungsten based catalyst and 2.85% wt. for the niobium based catalyst after 450°C indicates an extended process of gradual loss of hydroxyl groups from the crystalline structure of the metal/alumina/zeolite[27]. Based on the TGA/DTG profile, a temperature of 450°C was chosen for the calcination of the catalysts. The appearance of particle agglomerations was evaluated by scanning electron microscopy (SEM) as can be seen in the figures 5-7.

The scanning electron microscopy (SEM) images of the catalysts reveal that the particles are uniformly dispersed, at low concentrations, throughout the mass of γ-Al2O3-ZSM-5. SEM image analysis revealed that the average size of the agglomerates was usually between 900 and 2000.

Catalysts activity evaluation

The activity of W/Pd/γ-Al_2O_3-ZnZSM5 and Nb/Pd/γ-Al_2O_3-ZnZSM5 catalysts in the hydrodeoxygenation-hydrocracking of methyl esters of fatty acids was high in the range of temperatures and pressures studied. Thus, figure 8 shows the influence of temperature on the conversion of methyl esters at a pressure of 20 bar and the influence of pressure on the conversion of methyl esters at a temperature of 300°C. The process proceeded with the formation of different classes of compounds in the liquid phase, such as n-aliphatic hydrocarbons, iso-aliphatic hydrocarbons, cycloaliphatic hydrocarbons, and arenes. No oxygenated organic compounds were identified in the collected liquid phase. The high efficiency of the two catalysts in the deoxygenation process of methyl esters of fatty acids at relatively mild operating conditions (temperatures of 300-380°C and pressures of 20-60 bar) is probably attributed to the presence of ZnZSM5 type zeolite.

`The yield of n-aliphatic hydrocarbons showed relatively high values (up to 95%) within the studied temperature and pressure range. At a pressure of 20 bar and lower temperature values (300-325°C), the W/Pd/γ-Al_2O_3-ZnZSM5 catalyst favored higher yields of n-aliphatic hydrocarbons compared to the Nb/Pd/γ-Al_2O_3-ZnZSM5 catalyst. However, at higher temperature values (350-380°C), the Nb/Pd/γ-Al_2O_3-ZnZSM5 catalyst achieved higher yields of n-aliphatic hydrocarbons. Additionally, for the pressure of 20 bar, increasing the temperature led to a decrease in the yield of n-aliphatic

hydrocarbons for both catalysts. This decrease is attributed to the increased reactivity of n-aliphatic hydrocarbons in processes such as isomerization, cyclization, and dehydro-aromatization with rising temperature. N-aliphatic hydrocarbons act as intermediates in the production of these classes of organic compounds. The decrease in n-aliphatic hydrocarbons yield with increasing temperature is more pronounced for the W/Pd/γ-Al_2O_3-ZnZSM5 catalyst, likely due to the higher concentration of Bronsted acid centers in this catalyst, which catalyze the isomerization and cyclization reactions of n-aliphatic hydrocarbons.

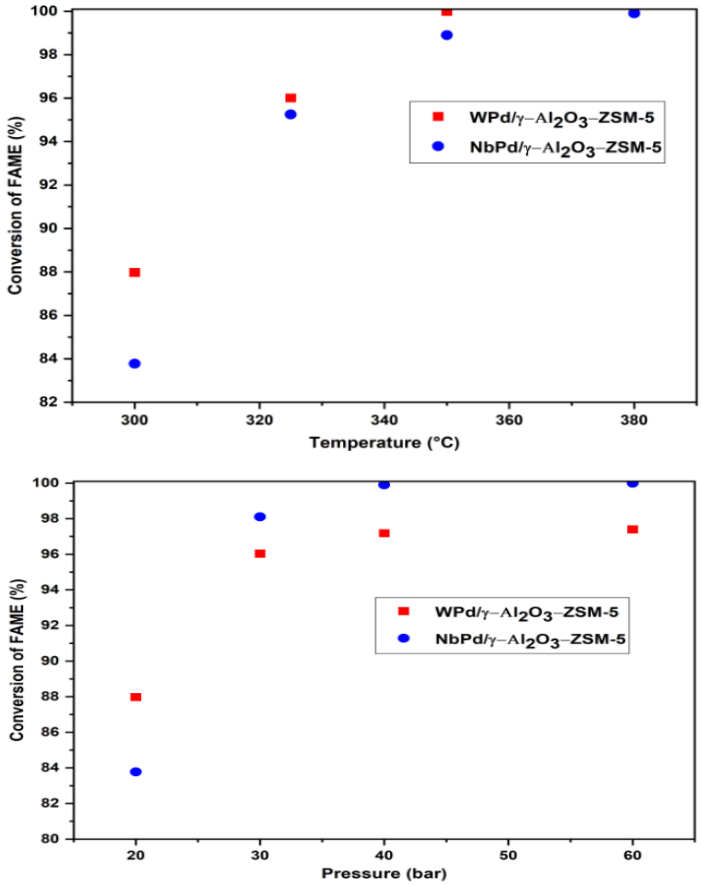

Figure 8. Conversion of fatty acid methyl esters (FAME) with temperature and pressure

The yield of n-aliphatic hydrocarbons with pressure at a temperature of 300°C varied following a curve with a minimum located at 30 atm for the Nb/Pd/γ-Al_2O_3-ZnZSM5 catalyst and at 40 atm for the W/Pd/γ-Al_2O_3-ZnZSM5 catalyst. This behavior is likely due to the fact that n-aliphatic hydrocarbons, as reaction intermediates, are formed through cracking reactions and are consumed in the isomerization-cyclization reaction at different rates at different pressures. At relatively low-pressure values (20-30 bar), the formation of n-aliphatic hydrocarbons is favored by improved adsorption on acidic centers. The increase in pressure above 40 bar disfavors the isomerization reactions of aliphatic hydrocarbons which are carried out by β-elimination reactions of carbocation type intermediates, thus reducing the consumption of such hydrocarbons.

In the studied temperature and pressure range, the yield of iso-aliphatic hydrocarbons, which are intermediates in the production of cycloaliphatic hydrocarbons, was lower compared to the yield of n-aliphatic hydrocarbons. At a pressure of 20 bar, the variation in iso-aliphatic hydrocarbons yield showed a maximum at 325°C for both studied catalysts. This behavior is likely due to the increased occurrence of pericyclic reactions of iso-aliphatic hydrocarbons at temperatures above 325°C, especially cycloaddition reactions, which proceed thermally and are favored by higher temperatures. As a result, the carboxyl group can activate any adjacent alkenic group (activated diene), promoting Diels-Alder reactions at relatively lower temperatures. The lower maximum yield of iso-aliphatic hydrocarbons on the W/Pd/γ-Al_2O_3-ZnZSM5 catalyst (26.1%) compared to the Nb/Pd/γ-Al_2O_3-ZnZSM5 catalyst (34.7%) is likely due to a more optimal distribution of Bronsted acid centers on the Nb/Pd/γ-Al_2O_3-ZnZSM5 catalyst. In this case, water formed during the deoxygenation process of the raw materials (methyl esters of fatty acids) reacts with WO_3type Lewis acids, favoring the formation of a larger quantity of Bronsted acids with lower strength, whose catalytic activity in isomerization reactions is reduced. Nb_2O_5-type Lewis acids do not react with the water formed in the deoxygenation process, and thus, the presence of water does not influence the concentration and strength of Bronsted acid centers and, consequently, the isomerization process for this catalyst.

The yield of iso-aliphatic hydrocarbons with pressure at a temperature of 300°C varied, with a maximum located at 30 atm for both catalysts, and a higher maximum value observed for the Nb/Pd/γ-Al_2O_3-ZnZSM5 catalyst (36.2%) compared to the W/Pd/γ-Al_2O_3-ZnZSM5 catalyst (31.6%). The decrease in iso-aliphatic hydrocarbons yield at pressure values higher than 30 bar is likely due to a reduction in β-elimination of the carbocation intermediates and the promotion of cycloaddition reactions of unsaturated intermediates

with increasing pressure. The higher yield of iso-aliphatic hydrocarbons on the Nb/Pd/γ-Al_2O_3-ZnZSM5 catalyst compared to the W/Pd/γ-Al_2O_3-ZnZSM5 catalyst is attributed to a more optimal distribution of Bronsted acid centers. Additionally, the abrupt drop to zero in the iso-aliphatic hydrocarbons yield at a pressure of 60 bar on the W/Pd/γ-Al_2O_3-ZnZSM5 catalyst is probably due to a reduction in the concentration of strong Bronsted acid centers resulting from the reaction of the WO_3Lewis acid with water formed during the deoxygenation of fatty acid esters. The adsorption of water on acid centers is favored by increasing pressure.

The yield of cycloaliphatic hydrocarbons showed average values (up to 29%) within the studied temperature and pressure range. On the W/Pd/γ-Al_2O_3-ZnZSM5 catalyst, cycloaliphatic hydrocarbons were not obtained at a pressure of 20 bar and lower temperature values (300°C). Increasing the temperature favored an increase in the yield of cycloaliphatic hydrocarbons, reaching up to 30% at a temperature of 380°C. Similarly, for the Nb/Pd/γ-Al_2O_3-ZnZSM5 catalyst, the yield of cycloaliphatic hydrocarbons increased with temperature within the studied temperature range, with the increase becoming less pronounced at higher temperatures (380°C). This increase is due to pericyclic reactions, such as cycloaddition reactions of dienes with activated dienes, which are compounds formed from the cracking of fatty acid esters; the exothermic nature of the cycloaddition reactions reduces this process at high temperatures.

For the Nb/Pd/γ-Al_2O_3-ZnZSM5 catalyst, at a temperature of 300°C, the yield of cycloaliphatic hydrocarbons increased with increasing pressure; however, the increase becomes insignificant at pressures above 30 bar. On the other hand, for the W/Pd/γ-Al_2O_3-ZnZSM5 catalyst, the increase followed a curve with a maximum, and as a result, cycloaliphatic hydrocarbons were not identified at pressures of 20 bar and 60 bar. The absence of cycloaliphatic hydrocarbons at a pressure of 20 bar is likely due to reduced accessibility in the pores that allow the occurrence of pericyclic reactions (shape selectivity). The absence of cycloaliphatic hydrocarbons at higher pressures (above 60 bar) is probably due to the negative influence of pressure on the β-elimination reactions of carbocations, which are intermediates in the cracking and isomerization process; the absence of iso-aliphatic hydrocarbons supports this conclusion. Pressure values of 30-40 bar favor the β-elimination reactions of carbocations, which lead to the formation of cycloaliphatic and iso-aliphatic hydrocarbons.

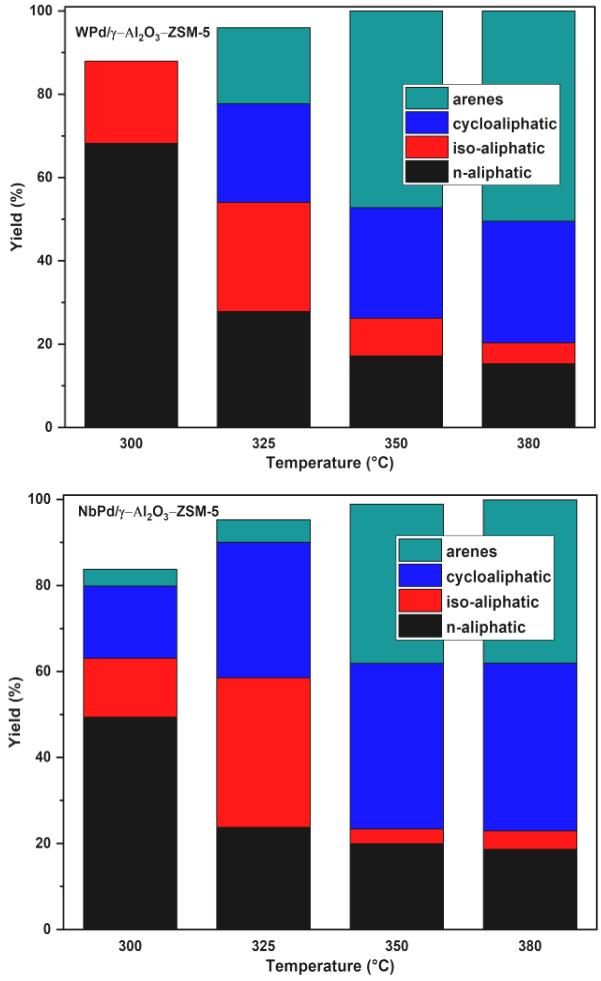

Figure 9. The yield in hydrocarbons with temperature, at pressure 20 bar, LHSV 0.5 h^{-1} for both catalysts

The yield of arenes reached values of up to 51% within the studied temperature and pressure range. On the W/Pd/γ-Al_2O_3-ZnZSM5 catalyst, arenes were not obtained at a pressure of 20 bar and lower temperature values (300°C), indicating that arenes are formed through the dehydrogenation of cycloaliphatic hydrocarbons (which were also not obtained at these parameter values). Increasing the temperature favored an increase in the yield of arenes, reaching up to 50.5% at a temperature of 380°C.

Similarly, for the Nb/Pd/γ-Al_2O_3-ZnZSM5 catalyst, the yield of arenes increased with increasing temperature within the studied temperature range, and the increase became less pronounced at higher temperatures (380°C), similar to the behavior observed for the W/Pd/γ-Al_2O_3-ZnZSM5 catalyst. This behavior is due to the dehydrogenation reactions of cyclic intermediates obtained through pericyclic reactions, such as the Diels-Alder 4+2 cycloaddition reactions of dienes with activated dienes. The tendency of decreasing slopes in the yield variation curves of arenes at temperatures of 350-380°C is attributed to the exothermic nature of the dehydrogenation reaction of alkyl-cyclohexadiene intermediates obtained through Diels-Alder reactions, which becomes unfavorable with increasing temperature.

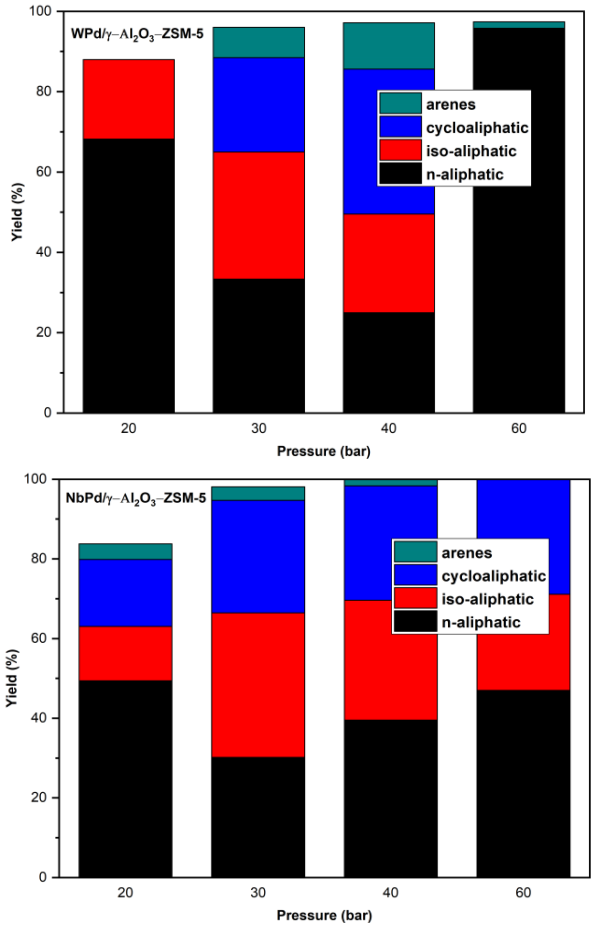

Figure 10. The yield in hydrocarbons with pressure, at 300°C, LHSV 0.5h^{-1} for both catalysts

For the Nb/Pd/γ-Al_2O_3-ZnZSM5 catalyst, at a temperature of 300°C, the yield of arenes decreased with increasing pressure, and the decrease became more pronounced at pressures above 30 bar, with the yield of arenes reaching zero at 60 bar. On the W/Pd/γ-Al_2O_3-ZnZSM5 catalyst, the yield of arenes varied following a curve with a maximum located at a pressure of 40 bar, so at a pressure of 20 bar, no arenes were identified, and at 60 bar, the yield of arenes was approximately 7 times lower than at 40 bar.

The absence of arenes on the W/Pd/γ-Al_2O_3-ZnZSM5 catalyst at a pressure of 20 bar and a temperature of 300°C is most likely due to the absence of cycloaliphatic hydrocarbons. The absence or reduced concentration of arenes at high pressures is due to the unfavorable dehydrogenation process with increasing pressure (a process that proceeds with an increase in the number of moles). The higher yields of arenes on the W/Pd/γ-Al_2O_3-ZnZSM5 catalyst compared to the Nb/Pd/γ-Al_2O_3-ZnZSM5 catalyst at pressures of 30-40 bar highlight the contribution of acid centers in the dehydrogenation process of cycloaliphatic hydrocarbons.

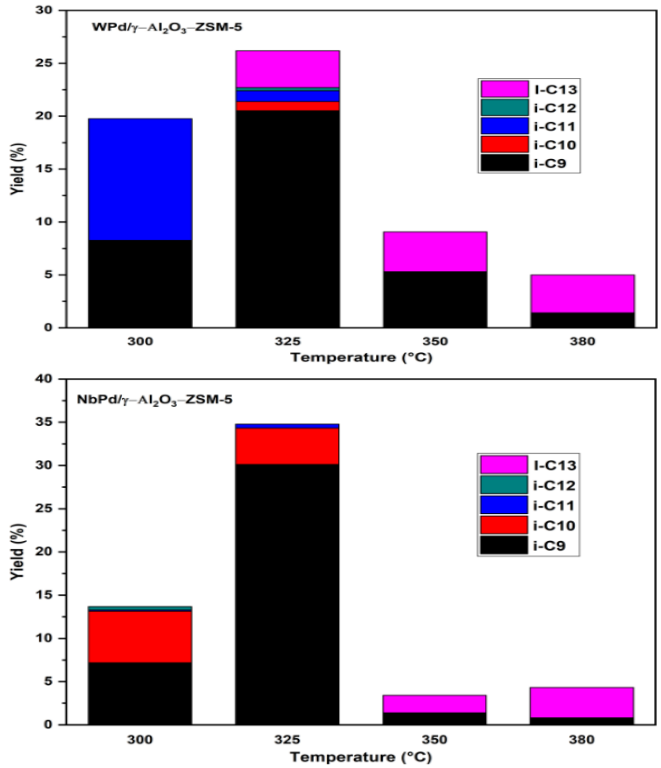

Figure 11. The yield in iso-aliphatic hydrocarbons with temperature, at pressure 20 bar, LHSV 0.5 h^{-1} for both catalysts

The influence of pressure on the yield of n-aliphatic hydrocarbons differed for the two catalysts. For the Nb/Pd/γ-Al_2O_3-ZnZSM5 catalyst, the yield of n-C10 to n-C13 increased with pressure, while the yield of n-C15 to n-C18 decreased with increasing pressure. For the W/Pd/γ-Al_2O_3-ZnZSM5 catalyst, the yield of n-C10, n-C11, n-C15, n-C17, and n-C18 varied with pressure following a curve with a minimum. However, the yield of n-C12 and n-C13 increased with pressure, while the yield of n-C16 varied with pressure following a curve with a maximum. Additionally, the yield of n-C18 tended to approach the yield of n-C17 at pressures higher than 60 bar, demonstrating that the hydrodeoxygenation process through decarboxylation is disfavored at high pressures.

The identified aromatic hydrocarbons in the liquid reaction product were arenes-C8 and arenes-C9 for both tested catalysts. The yield of arenes-C8 was higher than that of arenes-C9 over the entire range of variation of parameters for both catalysts studied. Generally, at a pressure of 20 bar, the yield of arenes increased with temperature for the Nb/Pd/γ-Al_2O_3-ZnZSM5 catalyst. For the W/Pd/γ-Al_2O_3-ZnZSM5 catalyst, the yield of arenes-C8 increased with temperature over the temperature range of 325°C to 380°C at the same pressure, while the content of arenes-C9 varied following a curve with a maximum. Overall, the yield of arenes was higher on the W/Pd/γ-Al_2O_3-ZnZSM5 catalyst compared to the Nb/Pd/γ-Al_2O_3-ZnZSM5 catalyst.

The yield of arenes-C8 varied with pressure following a curve with a maximum for both tested catalysts at a temperature of 300°C. The low values of the yield of both arenes at high pressures are attributed to the negative influence of high pressures on processes involving an increase in the number of moles. The Nb/Pd/γ-Al_2O_3-ZnZSM5 catalyst did not produce arenes-C9 at pressures above 20 bar, while the W/Pd/γ-Al_2O_3-ZnZSM5 catalyst showed a decrease in the content of these arenes with increasing pressure.

For both tested catalysts, the identified iso-aliphatic hydrocarbons in the liquid reaction product were iso-C9 to iso-C13. Generally, at a pressure of 20 bar and lower temperatures (300°C to 325°C), higher yields of iso-C9 were obtained for both catalysts, while increasing the temperature to values above 350°C favored the formation of iso-C13 hydrocarbons. The Nb/Pd/γ-Al_2O_3-ZnZSM5 catalyst showed higher yields of iso-C9 compared to the W/Pd/γ-Al_2O_3-ZnZSM5 catalyst, likely due to an optimal distribution of acidic strength (the acidic strength of WO_3 centers diminishes in the presence of adsorbed water in the catalytic pores, while the acidic strength of Nb_2O_5 centers remains unchanged in the presence of water). The decrease in the yield of iso-aliphatic hydrocarbons with increasing temperature (except for iso-C13) can be attributed to their tendency to cyclize at temperatures above 325°C in the presence of acidic catalysts.

The yield of iso-C9 varied with pressure following a curve with a maximum for both tested catalysts at a temperature of 300°C. Increasing the pressure above 30 bar unfavorably affected the elimination reactions of carbocation intermediates and, consequently, the isomerization reactions. The yield of iso-C10 to iso-C13 was not significantly influenced by increasing pressure and generally remained below 1% over the studied pressure range for both catalysts, except for the yield of iso-C11 on the W/Pd/γ-Al_2O_3-ZnZSM5 catalyst, which ranged from 2% to 11%.

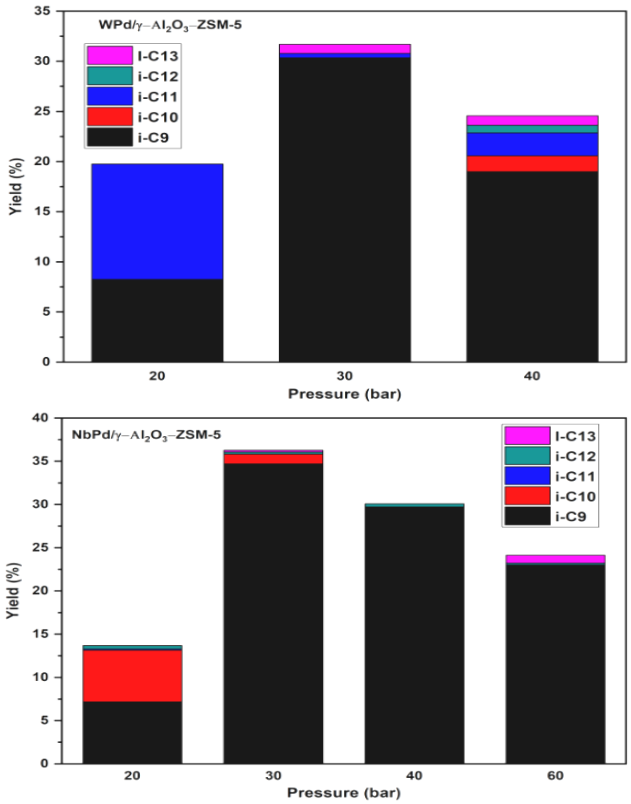

Figure 12. The yield in iso-aliphatic hydrocarbons with pressure, at 300°C, LHSV 0.5 h^{-1} for both catalysts

The cyclo-aliphatic hydrocarbons identified in the liquid reaction product were cyclo-C8 and cyclo-C9 for both tested catalysts. This information highlights the high reactivity of the ZnZSM5 zeolite in the cyclization reaction of n- and iso-C8 hydrocarbons, which were not detected in the reaction product, indicating that they cyclized instantaneously after formation. For the Nb/Pd/γ-Al_2O_3-ZnZSM5 catalyst, the yield of cyclo-C8 varied with temperature

following a curve with a maximum located at 325°C at a pressure of 20 bar. The W/Pd/γ-Al_2O_3-ZnZSM5 catalyst exhibited lower performance than the Nb/Pd/γ-Al_2O_3-ZnZSM5 catalyst at a pressure of 20 bar, and the yield of cyclo-C8 decreased with increasing temperature over the temperature range of 325°C to 380°C. On the other hand, the yield of cyclo-C9 increased with temperature over the temperature range of 300°C to 380°C for both catalysts. The porous structure of ZnZSM5 likely favors the formation of intermediates such as n- and iso-C9 hydrocarbons over n- and iso-C8 hydrocarbons.

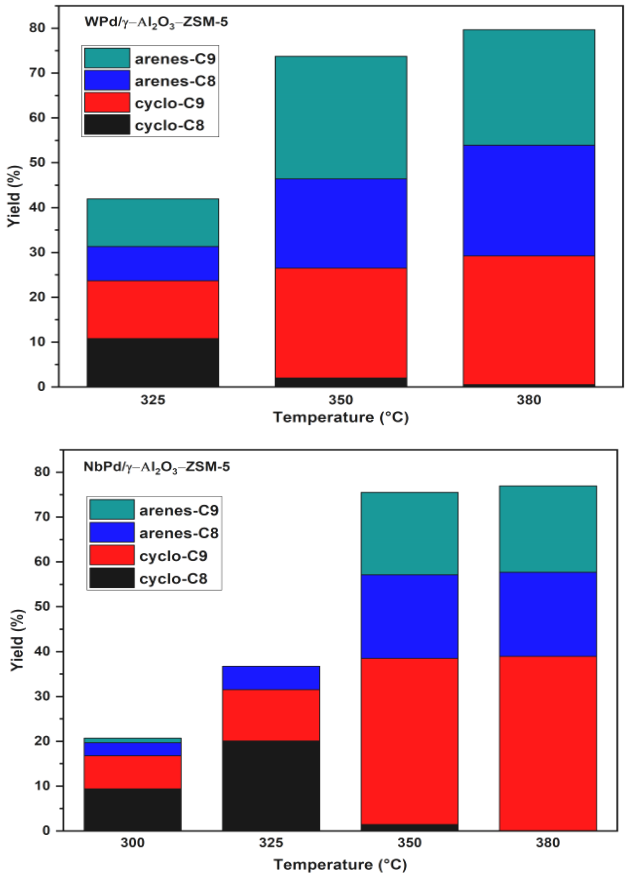

Figure 13. The yield in C8 and C9 cyclo-aliphatic hydrocarbons with temperature, at pressure 20 bar, LHSV 0.5 h^{-1} for both catalysts

The yield of cyclo-aliphatic hydrocarbons C8 varied with pressure following a curve with a maximum for both tested catalysts at a temperature of 300°C. The W/Pd/γ-Al_2O_3-ZnZSM5 catalyst exhibited a higher maximum

yield in cyclo-C8 compared to the Nb/Pd/γ-Al_2O_3-ZnZSM5 catalyst (approximately 25% compared to 17%). The abrupt decrease in the yield of cyclo-C8 and cyclo-C9 to 0% at a pressure of 60 atm in the case of the W/Pd/γ-Al_2O_3-ZnZSM5 catalyst is likely due to the decrease in Bronsted acidic strength of WO_3 centers in the presence of water resulting from the deoxygenation reaction, with water adsorption favored at high pressures. In contrast, an increase in the yield of cyclo-C9 with pressure was observed for the Nb/Pd/γ-Al_2O_3-ZnZSM5 catalyst over the entire studied pressure range.

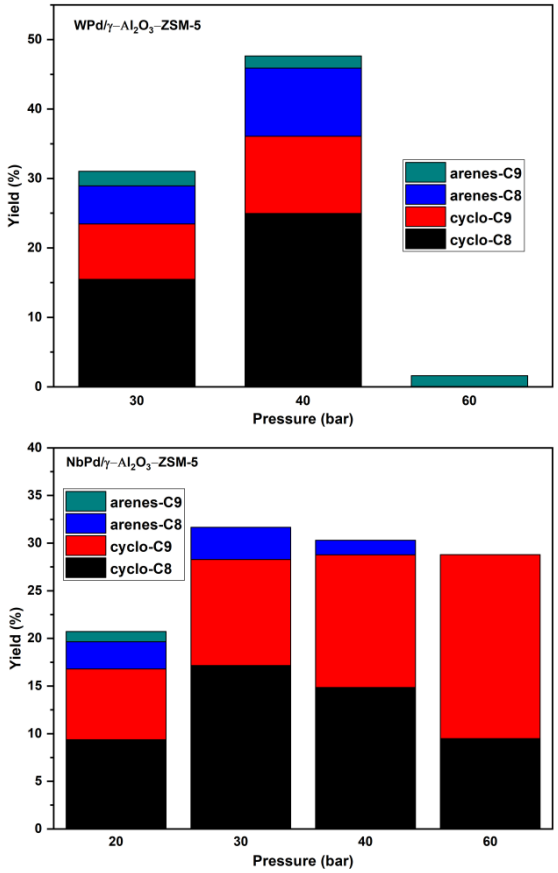

Figure 14. The yield in C8 and C9 cyclo-aliphatic hydrocarbons with pressure, at 300°C, LHSV 0.5 h^{-1} for both catalysts

The identified n-aliphatic hydrocarbons in the liquid reaction product were n-C10, n-C11, n-C12, n-C13, n-C15, n-C16, n-C17, and n-C18. Among these n-aliphatic hydrocarbons, n-C10, n-C15, n-C16, and n-C17 showed high yields at a temperature of 300°C and a pressure of 20 bar (ranging from

5% to 31% for both tested catalysts, with the W-based catalyst exhibiting higher yields for n-C10). However, with increasing temperature above 325°C, the yields of these hydrocarbons decreased rapidly, and at 380°C, except for n-C15, the yield became zero.

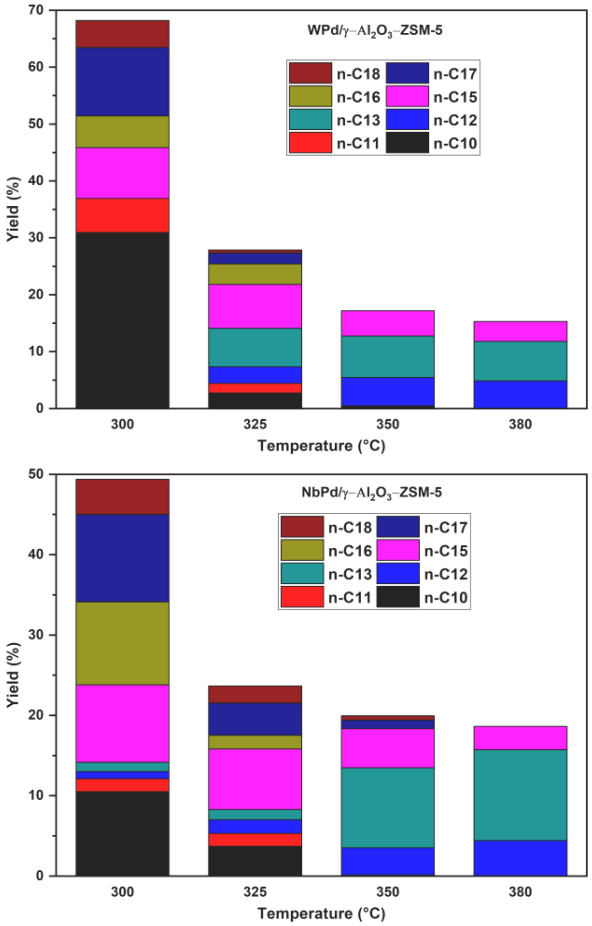

Figure 15. The yield in n-aliphatic hydrocarbons with temperature, at pressure 20 bar, LHSV 0.5 h^{-1} for both catalysts

On the other hand, n-C11, n-C12, and n-C13 exhibited lower yields at 300°C and 20 bar (ranging from 6% to 0%). But, with increasing temperature above 325°C, the yield variation for n-C11, n-C12, and n-C13 differed, resulting in relatively higher yields (4.4% and 11.3% for the Nb-based catalyst, and 4.8% and 6.9% for the W-based catalyst) at 380°C. The yield of n-C18 was approximately half of that for n-C17 throughout the studied

temperature range, indicating that deoxygenation proceeds with approximately 33% by the hydrogenation of the carboxylic bond and approximately 67% by decarboxylation. The absence of n-aliphatic hydrocarbons with less than 10 carbon atoms is likely due to their higher tendency for cyclization and dehydrogenation.

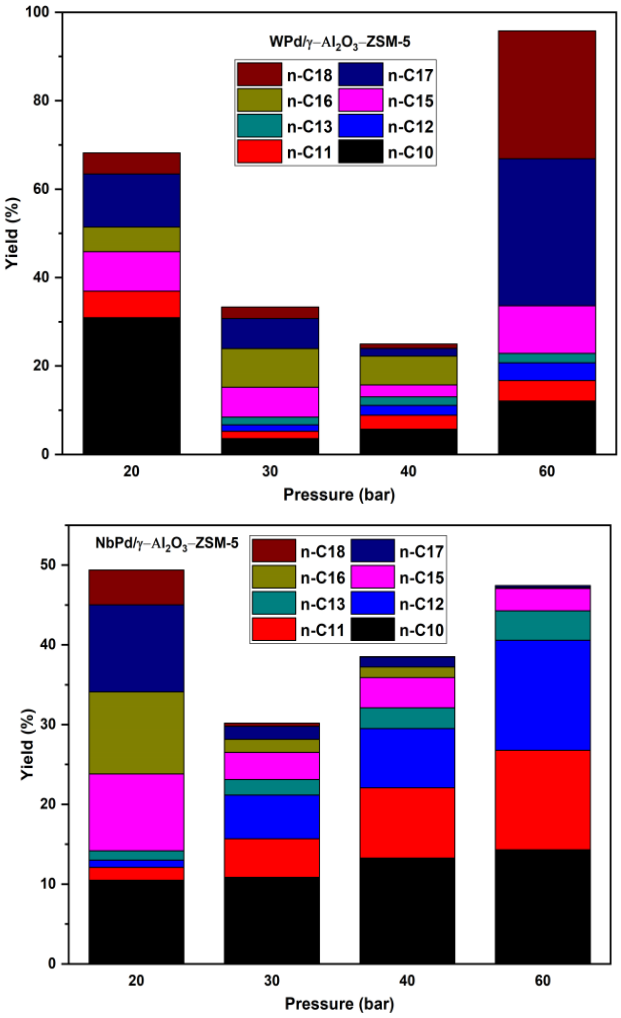

Figure 16. The yield in n-aliphatic hydrocarbons with pressure, at 300°C, LHSV 0.5 h^{-1} for both catalysts

CONCLUSIONS

The W-based catalyst exhibited higher activity than the Nb-based catalyst, attributed to a higher concentration of Lewis-type acidic centers (over 92%) and Bronsted-type acidic centers (close to 50%).

The hydrodeoxygenation-hydrocracking process of methyl esters of fatty acids on the W/Pd/γ-Al_2O_3-ZnZSM5 and Nb/Pd/γ-Al_2O_3-ZnZSM5 catalysts at 300-380°C and 20-60 bar resulted in the formation of different classes of hydrocarbons in the liquid phase, such as n-aliphatic hydrocarbons, iso-aliphatic hydrocarbons, cycloaliphatic hydrocarbons, and arenes.

Increasing the pressure to over 30-40 bar unfavorably affected the isomerization reactions by reducing the β eliminations to the intermediate carbocations, leading to a decrease in the consumption of n-aliphatic hydrocarbons. Thus, the yield of iso-aliphatic hydrocarbons, intermediates in the process of obtaining cycloaliphatic hydrocarbons, was lower compared to the yield of n-aliphatic hydrocarbons.

The high activity in the cyclization process of the catalysts tested over the range of parameters studied is probably due to the presence of the carboxyl group that can activate a nearby alkene group, favoring the occurrence of Diels-Alder reactions at relatively lower temperature values.

Over the studied temperature range at lower pressure, the yield of n-C18 remained constant, approximately half of the yield of n-C17, indicating that deoxygenation occurs to approximately 33% through the hydrogenation of the carboxylic bond and to approximately 67% through decarboxylation/ decarbonylation. Additionally, the yield of n-C18 tends to approach the yield of n-C17 at higher pressure values of over 60 bar, indicating that at high pressures, the decarboxylation process is less favored in the hydrodeoxygenation process.

EXPERIMENTAL SECTION

Characterization of palm oil fatty acids methyl esters

Synthesis of fatty acids methyl esters was described in a previous work [28]. The analysis of fatty acids methyl esters and of the reaction products was carried out using a GC–MS TRIPLE QUAD (Agilent 7890 A) with a DB-WAX capillary column (30 mL, 0.25 mm internal diameter, 0.25 μm film thickness). Helium was the carrier gas with a flow rate of 1 mL/min. The oven temperature was set at 70 °C and was increased to 230 °C with a rate of 4 °C / minute

with 5 minutes holding time. The GC injector and MS ion source temperatures were set at 250 °C and 150 °C, respectively. Transfer line temperature was set at 280 °C. The MS detector was operated in EI mode at 70 eV, with a m/z scanning range of 50–450. Peaks were identified using a NIST MS database [29]. The distribution of fatty acid methyl esters was as follows: methyl myristate (1.51 wt.%), methyl palmitate (35.72 wt.%), methyl stearate (6.68 wt.%), methyl oleate (41.82 wt.%), methyl linoleate (13.6 wt.%) and methyl icosanoate (0.66 wt.%) [16].

Catalysts preparation

The catalyst support is a mixture of 70% powdery γ-alumina (VGL-25 type, UOP Versal, Honeywell) and 30% ZnZSM-5. In the first step, 2.9 liters of deionized water, 570 grams of silica-alumina with a SiO_2/Al_2O_3 ratio of 125, 200 grams of melted hexamethylenediamine, and 20 grams of zinc acetate dissolved in 100 ml of water were added to a 10-liter stirred autoclave. The pH of the suspension was adjusted using a 50% NaOH solution to a value of 12.2, and then it was heated to 174°C under stirring for 48 hours. The pressure in the autoclave reached 9 bars. After 48 hours, the synthesized mixture was transferred to a stainless-steel autoclave with a Teflon-coated surface and dried at 120°C for 24 hours, followed by crystallization for 12 hours at 170°C. The obtained product was centrifuged, washed with distilled water until it reached a pH of 7, then dried at 120°C for 12 hours and calcined at 550°C for 10 hours. 250 grams of the obtained zeolite with MFI structure, was mixed with 2 liters of 10% ammonium nitrate solution and deionized water in a stirred vessel at 95°C for 2 hours. The operation was repeated twice. After centrifugation, the ammonium form of the zeolite was washed with 7 liters of deionized water, and the obtained suspension was centrifuged again, then the resulting zeolite was dried at 120°C for 12 hours [30].

The second stage of preparing the catalytic support involved mixing 70% γ-Al_2O_3 (type VGL-25, UOP Versal, Honeywell) and 30% ZnZSM-5 in powder form in a 1-liter capacity horizontal mixer with a heating mantle, along with a solution of nitric acid (HNO_3, 10% mass), which was gradually dosed over 60 minutes. After dosing the HNO_3 solution, mixing continued at room temperature for 4 hours. A homogeneous paste was obtained and introduced into an automatic extruder with a nozzle diameter of 1 mm. By extrusion, cylindrical granules were obtained, which were dried for 8 hours at a temperature of 150°C. After drying, the cylindrical extrudate catalytic support was calcined at a temperature of 450°C, with a heating rate of $5°C \cdot min^{-1}$ [30].

Two catalysts were prepared by impregnating the extruded catalytic support with aqueous solutions of metal precursors [18,31-33]. Thus, a W/Pd/γ-Al_2O_3-ZnZSM-5 catalyst was prepared by successive impregnation

with ammonium tungstate solution and palladium nitrate respectively at a concentration of 6.5%W and 1%Pd, and a Nb/Pd/γ-Al_2O_3-ZnZSM-5 catalyst was prepared by successive impregnation with a solution of niobium oxalate and palladium nitrate respectively at a concentration of 6.5%Nb and 1%Pd. Both catalysts were then dried at 250°C for 3 hours, following which each catalyst was impregnated with a solution of palladium nitrate (II) dihydrate (40% Pd) - $Pd(NO_3)_2 \cdot 2H_2O$ (Sigma Aldrich) in water. The impregnated catalysts were subsequently dried at 250°C for 3 hours. Before the experimental tests, the oxide precursors were reduced under a H_2 stream, at 250 °C and 5 bar for 2 hours; then, the temperature was increased to 450 °C, and the activation continued for 8 hours [16,19].

Catalysts characterization

Textural characteristics of the catalysts (surface area, pore volume, average pore diameter and pore-size-distribution) were measured by a Quantacrome NOVA 2200e instrument, by physisorption of nitrogen at -196 °C.

Thermogravimetric analyses (TGA) of the catalyst were recorded on a TGA/-IST (Thermal Analysis System TGA 2, METTLER TOLEDO, Greifensee, Switzerland) in the 30–600 °C temperature range, in a nitrogen atmosphere, with a heating rate of 10 °C/min.

The acidic properties of the catalyst (the concentrations of Brønsted and Lewis acid sites) were evaluated through the pyridine-adsorbed FT-IR spectrum analysis of pyridine adsorption by the ring vibration of pyridine detected in the frequency range of 1420–1550 cm−1 and was recorded using Tracer-100 (Shimadzu Europa GmbH) Shimadzu Fourier-Transform Infrared Spectrophotometer with KBr pellet method.

Structural morphology images of the catalysts using a Scios 2 HIVAC Dual-Beam ultra-high-resolution FIB-SEM.

Catalytic reaction

Experimental tests were carried out in a fixed bed reactor (length of 50 cm, diameter of 2.25 cm). A catalyst volume of 40 cm^3 was loaded in the middle of the reactor and the top and the bottom were filled each with 80 cm^3 inert glass beads [34,35]. The liquid samples were analyzed by GC/MS 7000 Triple Quad MS (Agilent Technologies) system equipped with HP-FFAP (30 m, 250 μm, 0.25 μm) column and He as carrier gas with volumetric flow of 1 ml/min.

REFERENCES

1. Mortensen, P.M.; Grunwaldt, J.D.; Jensen, P.A.; Knudsen, K.G.; Jensen, A.D; *Appl. Catal. A: General*, **2011**, *407*, 1-19.
2. Di Vito Nolfi, G.; Gallucci, K.; Rossi, L; I J. Environ. Res. Public Healt, **2021**, 18.
3. Jamil, F.; Al-Haj, L.; Al-Muhtaseb, A.a.H.; Al-Hinai, M.A.; Baawain, M.; Rashid, U.; Ahmad, M.N.M; *Rev. Chem. Eng* **2018**, *34*, 267-297.
4. Li, J.; Zhang, J.; Wang, S.; Xu, G.; Wang, H.; Vlachos, D.G; *ACS Catalysis*, **2019**, *9*, 1564-1577.
5. Ray, P.; Clément, M.; Martini, C.; Abdellah, I.; Beaunier, P.; Rodriguez-Lopez, J.-L.; Huc, V.; Remita, H.; Lampre, I; New J. Chem., **2018**, *42*, 14128-14137.
6. Cao, Y.; Shi, Y.; Bi, Y.; Wu, K.; Hu, S.; Wu, Y.; Huang, S; *Fuel Process. Techn*., **2018**, *172*, 29-35.
7. Jing, Z.-Y.; Zhang, T.-Q.; Shang, J.-W.; Zhai, M.-l.; Yang, H.; Qiao, C.-Z.; Ma, X.-Q; *J. Fuel Chem.Technol*.,**2018**, *46*, 427-440.
8. Konwar, L.J.; Oliani, B.; Samikannu, A.; Canu, P.; Mikkola, J.-P; *Biomass Conv. Bioref*., **2022**, *12,* 51-62.
9. Cheng, J.; Zhang, Z.; Zhang, X.; Liu, J.; Zhou, J.; Cen, K; *Fuel*, **2019**, *245*, 384-391.
10. Nepomniashchii, A.A.; Buluchevskiy, E.A.; Koshevaya, Y.O.; Gulyaeva, T.I.; Lavrenov, A.V; AIP Conference Proceedings, **2020,** *2301*, 030013.
11. Hong, Y.-K.; Lee, D.-W.; Eom, H.-J.; Lee, K.-Y; *Appl. Catal. B: Environmental*, **2014**, *150-151*, 438-445.
12. Ardiyanti, A.R.; Gutierrez, A.; Honkela, M.L.; Krause, A.O.I.; Heeres, H.J; *Appl. Catal. A: General,* **2011**, *407*, 56-66.
13. Zerva, C.; Karakoulia, S.A.; Kalogiannis, K.G.; Margellou, A.; Iliopoulou, E.F.; Lappas, A.A.; Papayannakos, N.; Triantafyllidis, K.S; *Catal. Today*, **2021**, *366*, 57-67.
14. Shao, Y.; Xia, Q.; Liu, X.; Lu, G.; Wang, Y; *Chem Sus Chem*, **2015**, *8*, 1761-1767.
15. Srihanun, N.; Dujjanutat, P.; Muanruksa, P.; Kaewkannetra, P; *Catalysts*, **2020**, 10.
16. Marinescu, M.; Popovici, D.R.; Bombos, D.; Vasilievici, G.; Rosca, P.; Oprescu, E.-E.; Bolocan, I; Reaction Kinetics, *Mecha Catalysis*, **2021**, 133, 1013-1026.
17. Doukeh, R.; Bombos, M.; Bombos, D.; Vasilievici, G.; Radu, E.; Oprescu, E.-E; *React. Kinet., Mech. Catal.*, **2021**, *132*, 829-838.
18. Doukeh, R.; Leostean, C.; Bolocan, I.; Trifoi, A.R.; Banu, I; *Chem Select*, **2021**, *6*, 3858-3868.
19. Doukeh, R.; Bombos, D.; Bombos, M.; Oprescu, E.-E.; Dumitrascu, G.; Vasilievici, G.; Calin, C.; *Sci. Rep.*, **2021**, *11*, 6176.
20. Doukeh, R.; Juganaru, T.; Bolocan, I, *Revista de chimie*, **2019**, *70*, 3132-3135.
21. Zhang, X.; Lin, T.; Li, R.; Bai, T.; Zhang, G; *Ind. Eng. Chem. Res*., **2012**, *51*, 3541-3549.

22. Doukeh, R.; Râpă, M.; Matei, E.; Prodan, D.; Győrgy, R.; Trifoi, A.; Banu, I; *Catalysts*, **2023**, 13.
23. Aryee, E.; Dalai, A.K.; Adjaye, J; *Front. Chem. Eng*., **2022**, 3.
24. Kim, Y.; Moon, D; *Cat. Surveys Asia*, **2019**, 23.
25. Kristiani, A.; Sudiyarmanto, S.; Aulia, F.; Hidayati, L.; Abimanyu, H; MATEC Web of Conferences, **2017**, *101*, 01001.
26. Dippong, T.; Goga, F.; Avram, A; *Studia UBB Chemia*, **2017**, 62, 165-176.
27. Hermida, L.; *Journal of Materials and Environmental Sciences*, **2018**, *9*, 2328-2333.
28. Stepan, E.; Enascuta, C.-E.; Oprescu, E.-E.; Radu, E.; Radu, A.; Galan, A.-M.; Vasilievici, G.; Lavric, V.; Velea, S; *Fuel*, **2016**, *172*, 29-36.
29. Enascuta, C.E.; Stepan, E.; Bolocan, I.; Bombos, D.; Calin, C.; Oprescu, E.-E.; Lavric, V.; *Waste Management,* **2018**, *75*, 205-214.
30. Matei. V., Juganaru.T., Bombos. D., Borcea A. F., Marinescu C., Ganea R., Bombos M. M., OSIM, **2010**, RO 126664 A2.
31. Calin, C.; Leostean, C.; Trifoi, A.R.; Oprescu, E.-E.; Wiita, E.; Banu, I.; Doukeh, R., Scientific Reports **2021**, 11, 19053.
32. Doukeh, R.; Trifoi, A.; Bombos, M.; Banu, I.; Pasare, M.; Bolocan, I.O.N, *Rev. Chim*., **2018**, *69*, 396-399.
33. Dan, M.; Mihet, M.; Lazar, D.; Muresan, L. *Studia UBB Chemia*, **2016**, *61*, 137-154.
34. Oprescu, E.-E.; Enascuta, C.-E.; Doukeh, R.; Calin, C.; Lavric, V.;*Renewable Energy*, **2021**, *176*, 651-662.
35. Doukeh, R.; Bombos, M.; Bolocan, I.; *Rev. Chim.*, **2019**, *70*, 2481-248.